Reconstruction of high resolution ocean wind vectors from low resolution scatterometer measurements

David G. Long

Brigham Young University, 459 Clyde Building, Provo, UT 84602, USA

ABSTRACT

Designed to retrieve near-surface winds over the ocean, the SeaWinds scatterometer makes 13.4 GHz Ku-band measurements of the normalized radar backscatter of the Earth's surface from which the near-surface vector (speed and direction) wind is estimated. Conventional processing of the backscatter measurements results in 25 km resolution winds. However, by applying reconstruction algorithms the backscatter can be estimated at much finer resolution, albeit at reduced accuracy. This innovative application of reconstruction theory has a number of novel elements including irregular sampling, a two dimensional vector signal, multiplicative and additive noise, and a non-linear transfer function between the measurements and the signal. This paper describes the high resolution wind retrieval problem, the solution approaches adopted, and sample results.

Keywords: reconstruction, resolution enhancement, irregular sampling, scatterometer, SeaWinds, radar backscatter, ocean winds, QuikSCAT

1. INTRODUCTION

A wind scatterometer is a real-aperture radar designed to measure the normalized radar backscatter of the ocean's surface from space.[1] By making multiple backscatter measurements of the same location from different azimuth angles, the near-surface wind speed and direction can be determined with the aid of a geophysical model function relating wind and backscatter. In conventional processing, individual backscatter measurements at the same azimuth are gridded onto a uniform 25 km by 25 km grid, yielding nominally 25 km by 25 km resolution backscatter estimates for wind retrieval. Wind estimation non-linearly combines the measurements at different azimuth angles to estimate the wind with the resulting wind estimates having an effective resolution somewhat coarser than 25 km.

For some studies (notably in coastal areas), higher resolution wind estimates are desired. To this end, we utilize reconstruction techniques to compute the surface backscatter at higher resolution from which the wind is estimated at higher resolution. This problem is a rather interesting practical application of reconstruction theory and has a number of novel elements including irregular sampling, scalar measurements, a two dimensional vector signal (the wind), both multiplicative and additive noise sources, non-linear processing steps (wind estimation), and two different enhancement steps: an initial backscatter measurement enhancement and enhancement resulting from the wind estimation. A number of innovative techniques for signal enhancement were developed in solving this problem. This paper describes the problem and solution approaches, discussing theory, key tradeoffs and computational methods. Analysis, simulation and actual data are employed to validate the accuracy of the retrieved winds and evaluate the effective resolution of the wind estimates. Background is first provided in Section 2, followed by a description of the reconstruction-based processing in Section 3. Illustrations of the results are presented in Section 4 with a summary conclusion provided in Section 5.

Further author information:
DGL: E-mail: long@ee.byu.edu, Telephone: 1 801 422 4383

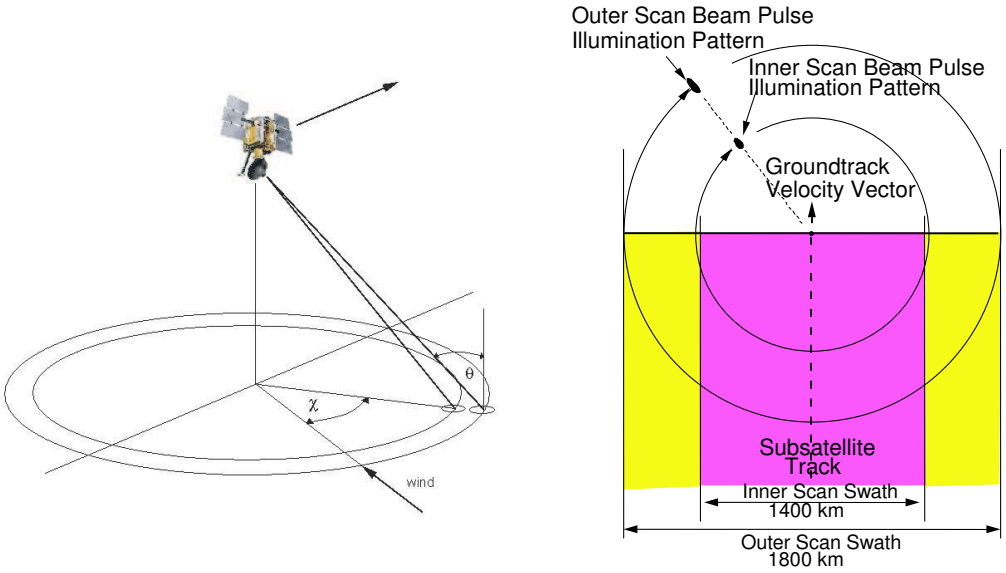

Figure 1. (left) SeaWinds orbital observation geometry. The dual pencil-beam antenna spins about nadir as the spacecraft moves along its orbit. (right) Illustration of the SeaWinds observation swath. For each point in the inner scan swath, measurements looking forward and backward from each beam (a total of four measurements) are collected. Over the outer scan, two measurements, one looking forward and one looking backward, are collected at each swath location.

2. BACKGROUND

The SeaWinds scatterometer was first launched in July 1999 aboard the QuikSCAT satellite. A second instrument was launched in December 2002 aboard the Japanese ADEOS-II satellite but operated for only 9 months before the spacecraft power system failed. The SeaWinds radar scatterometer is designed to measure the Ku-band (13.4 GHz) normalized radar backscatter (σ^o) of the Earth's surface at two incidence angles and two polarizations (H-pol at 46°, and V-pol at 54°) with a diversity of azimuth angles. From these measurements the near-surface vector wind can be estimated over the ocean.[1] SeaWinds σ° measurements over land and ice regions are useful in a variety of climate studies.[2]

The SeaWinds scatterometer transmits 0.5 ms microwave pulses at a pulse rate of 192 Hz using a dual-beam conically rotating dish antenna which rotates at approximately 18 rpm about the nadir vector. The radar transmits alternately on each of two beams. These beams trace out a helix on the earth as the satellite passes overhead.[3] The inner beam transmits and receives horizontally-polarized microwave signals while the outer beam transmits and receives vertically-polarized signals. Figure 1 illustrates the SeaWinds measurement geometry.[4]

The radar echo from the surface is received and processed to compute the σ° of the illuminated area.[5] The two-way 3 dB antenna footprint is elliptically shaped with dimensions of approximately 25 km by 35 km (see Fig. 2). The SeaWinds measurement of this area is termed an "egg". An onboard digital signal processor uses range filtering to divide the return echo into multiple range bins (termed "slices"), of which eight are retained and transmitted to the ground. The nominal operation mode results in slices with corresponding dimensions of approximately 6 km by 25 km.[3,5] Only slice measurements are used in the high resolution wind estimation described here.

The scanning and measurement geometry of SeaWinds results in irregular spacing of the individual measurements in the along-track and cross-track directions. In conventional processing the measurements are gridded onto a 25 km × 25 km grid. All the backscatter measurements whose center falls within a given grid element, known as a wind vector cell (wvc), are used to retrieve the wind at that wvc.

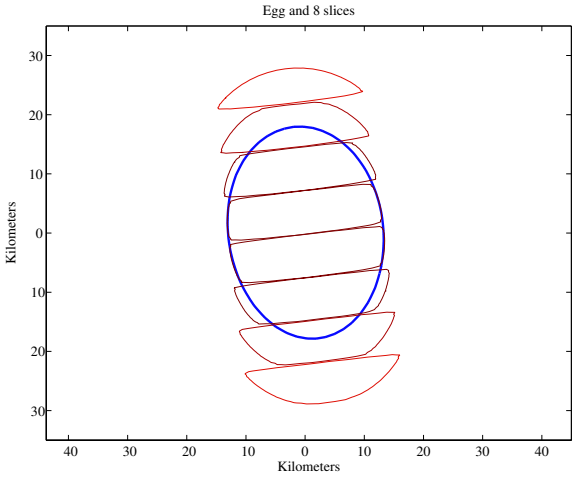

Figure 2. The 3 dB contours of the "egg" (thick line) and eight "slices" (thin lines) for a typical SeaWinds measurement. Compare with Fig. 2.

Over the inner swath each wvc is observed at least four times: twice by each beam, once when the beam is looking forward and once when the beam is looking aft as the spacecraft moves along track. Over the outer swath, measurements are from only two different azimuth angles. Measurements at different azimuth angles is an essential requirement for wind retrieval.[1]

For each wvc, the wind is estimated with the aid of a geophysical model function (GMF) which relates σ° to the vector wind,

$$\sigma^\circ = f(s, \phi - \chi, p, \theta)$$

where s is the wind speed, ϕ is the wind direction relative to north, χ is the look direction of the radar relative to north, p is the polarization of the radar signal (either horizontal or vertical), and θ is the incidence angle of the measurement. The relative azimuth angle between the radar look direction and the wind direction is $\psi = \phi - \chi$. The GMF is a tabular function, empirically estimated.[1] Figure 3 illustrates the GMF, plotting σ° versus the relative azimuth angle (ψ) at several wind speeds. As a function of ψ, σ° exhibits a $\cos 2\psi$ dependency.[1] Since σ° versus direction is non-unique, several σ° measurements collected at several azimuth angles are used to determine the wind direction. An example of wind estimation is illustrated in Fig. 4.

In reality, the simple wind estimation illustrated in Fig. 4 is more complicated because of noise which shifts the individual curves so they no longer intersect at the same point. The noise consists of both additive and multiplicative components.[7] Thus, a maximum-likelihood objective function is formulated and optimized to estimate the wind speed and direction.[1] Unfortunately, this estimate is also non-unique and results in from one to four wind vector estimates at each wvc.[1] These "ambiguities" have nearly the same wind speed, but differ in direction. To resolve the ambiguity, a separate, post-estimation step known as ambiguity selection is performed that selects a unique wind vector field to ensure spatial consistency in the wind at different wvcs.[1]

Standard 25 km resolution products are based on the egg measurements. Somewhat higher spatial resolution can be obtained by using slices rather than eggs when gridding the σ° measurements into wvcs; however, the resolution possible from gridding algorithms is limited to the largest dimension of the spatial response function since portions of the spatial response fall outside the grid element.[8]

3. HIGH RESOLUTION WIND ESTIMATION

Near-coastal studies, and studies of severe weather events require higher resolution wind estimates. With conventional processing, this is only possible if larger, more expensive antenna systems are used. However,

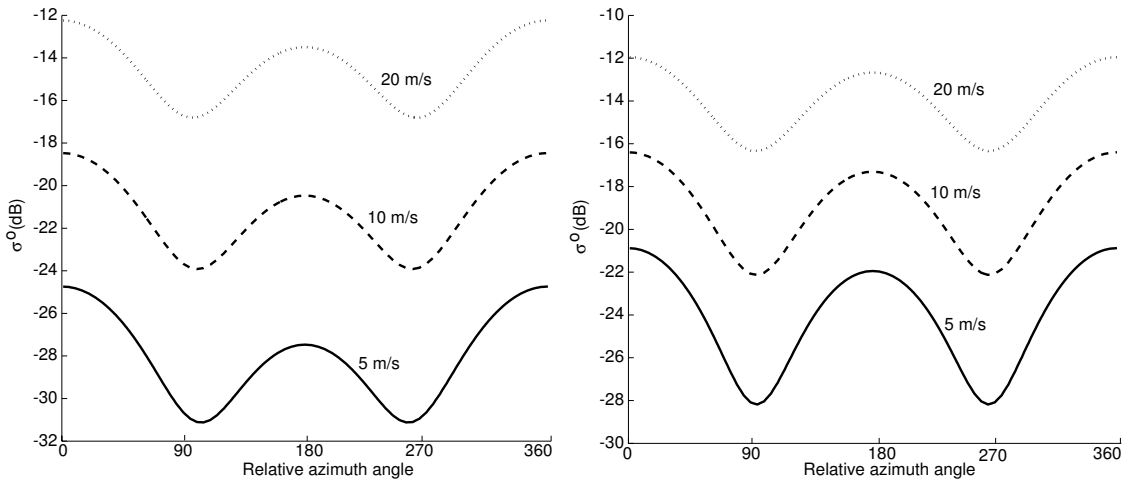

Figure 3. Plots of σ° versus relative azimuth angle $\phi - \chi$ between the wind direction and radar azimuth look direction for several wind speeds from the Ku-band geophysical model function at (left) 46° incidence angle, horizontal polarization, corresponding to the inner beam observations, and (right) 54° incidence angle, vertical polarization, corresponding to outer beam observations.[6]

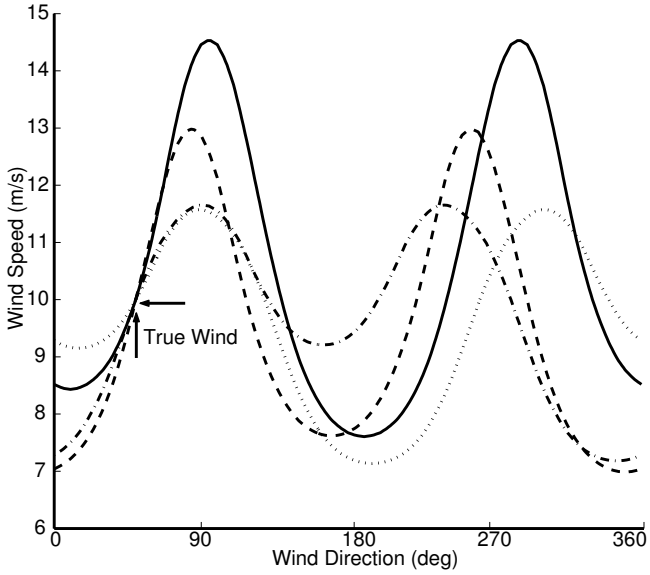

Figure 4. Simplified noise-free wind retrieval illustration. Individual lines represent the possible wind speeds and directions given the observed σ° from each of four colocated σ° measurements taken from different beams. The location in wind direction and wind speed where the curves intersect is the wind speed and direction estimate.

reconstruction techniques offer a method for higher resolution wind measurements from the existing SeaWinds instrument by exploiting the dense sampling and spatial overlap.

In considering reconstruction and resolution enhancement in connection with wind estimation, we first note that the signal of interest (the wind) is a vector quantity (speed and direction) while our observations (the σ° measurements) are scalar and noisy. Complicating our quest for higher resolution wind estimates is the both non-linear and non-unique relationship between σ° and the vector wind.

In this paper we adopt a simple approach to high resolution wind retrieval: we use reconstruction techniques to generate high spatial resolution estimates of the surface σ° separately for each azimuth look and then estimate the vector wind on a finely spaced grid using maximum-likelihood techniques. The σ° reconstruction provides part of the resolution improvement, while the combination of the azimuth looks in the wind estimation further improves the resolution. We note that the geometry of the rotating antennas and orientation of the slice measurement response results in variable effective resolution over the swath. Also, while the reconstruction provides improved spatial resolution, its high pass filter characteristics can also enhance the noise in the wind estimates. In the following subsections we consider the spatial response function of the individual σ° measurements, reconstruction theory, and wind retrieval. Sample results are presented.

3.1. The Scatterometer Spatial Response Function

The scanning and measurement geometry of the SeaWinds scatterometers results in irregular spacing of the individual measurements, which are densely spaced and exhibit significant spatial overlap. Combined in a reconstruction step and in wind retrieval, the dense sampling, along with the non-ideal roll-off of the spatial measurement response,[8] enables the reconstruction of σ° at finer resolution than gridding the observations. Key to the reconstruction is the spatial response function of the σ° measurements.

The measurement spatial response function (also known as the "point spread function" or the "aperture function") is the contribution of each point on the surface to the overall backscatter measurement. It is computed using the integral form of the radar equation[9] and is a function of the measurement geometry, the antenna gain pattern and the signal processing.[3] Derivation of the SeaWinds spatial response pattern is considered in detail in Ref.[4] Figure 5 illustrates the spatial response function for a typical egg and slice measurement (note that multiple slice measurements are collected simultaneously with each egg, see Fig. 2). We note that the effective spatial resolution of the reconstructed measurements has a thin aspect ratio, whose orientation varies with the azimuth angle of the observation. As the antenna rotates, the orientation of the slices varies over a 360° range.

For a given azimuth look, a particular σ° measurement $\hat{\sigma}^\circ_k$ can be written as convolution of the σ° of the surface $\sigma^\circ(x,y)$ with the spatial response function, $h_k(x,y)$, as

$$\hat{\sigma}^\circ_k = \iint h_k(x,y)\sigma^\circ(x,y)dxdy. \tag{1}$$

The unique measurement characteristics of scatterometers result in both additive and multiplicative noise in the measurements,[7] i.e. a noisy measurement z_k can be written as

$$z_k = \hat{\sigma}^\circ_k(1 + K_{pk}\nu_k) \tag{2}$$

where ν_k is a normally distributed gaussian random variable and K_{pk} is a quadratic function of the measurement signal-to-noise ratio, the coefficients of which are related to $\hat{\sigma}^\circ_k$.

Variations in the measurement geometry (e.g., due to the rotating antenna) result in a unique spatial response function ($h_k(x,y)$) for each measurement. Figure 6 illustrates the layout of slice measurements over a small area. Here the fore/aft slices are oriented nearly parallel; however, the slice orientation varies over the swath. In the mid-side swath, the so-called "sweet spot", they are nearly orthogonal, which results in the best wind resolution.

We also note from Fig. 6 that the spatial sampling is variable and irregular. Coupled with the varying response function, this precludes conventional deconvolution techniques for reconstructing σ°. It also imposes

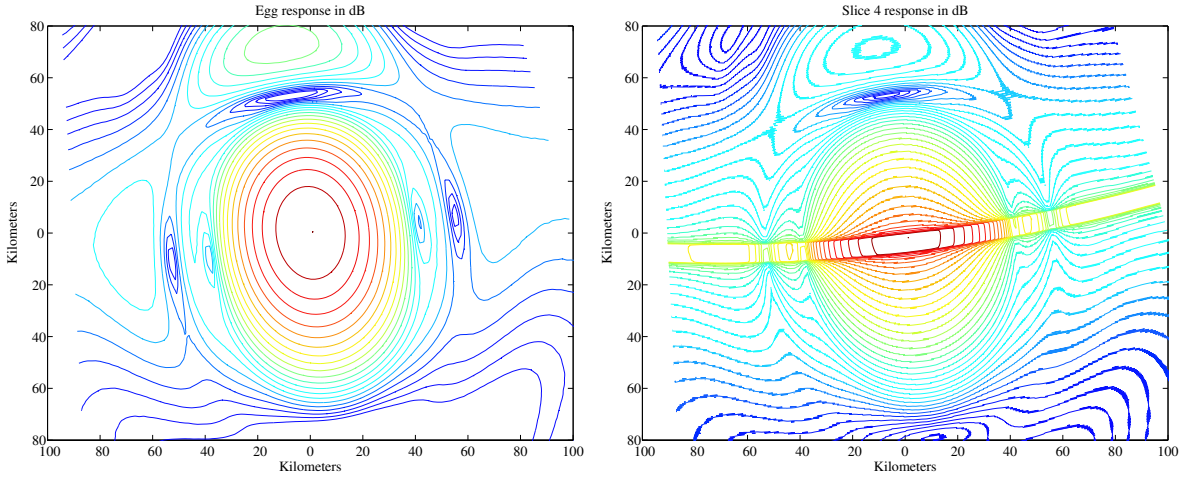

Figure 5. The spatial response function of a typical (left) "egg" and (right) "slice" measurement. (Multiple slice measurements are collected simultaneously, see Fig. 3.) The shapes and orientations of both slices and eggs vary with antenna azimuth angle and orbit position.[4] Contours are spaced at 3 dB with highest contour 3 dB down from the peak.

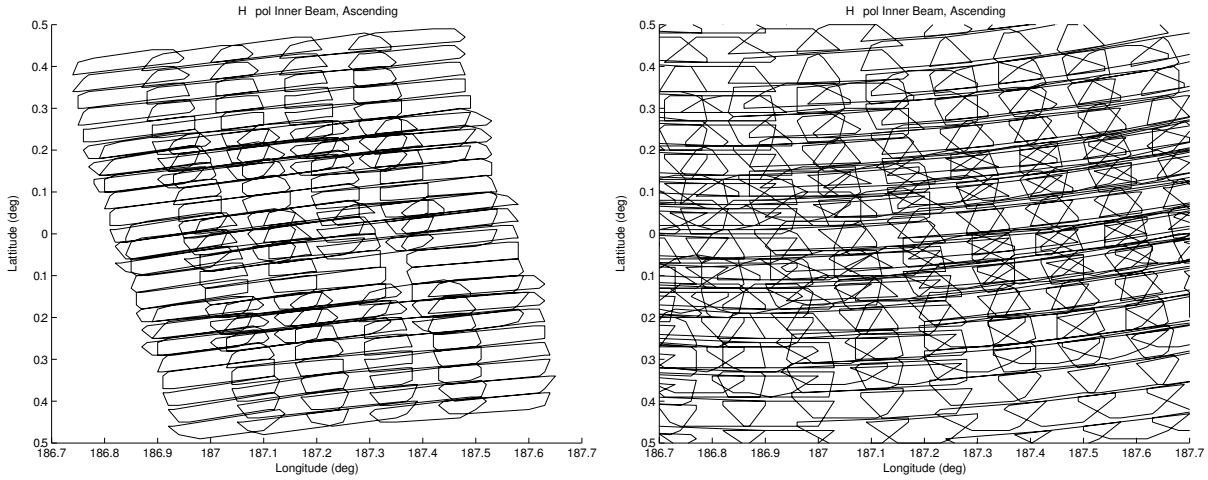

Figure 6. Illustration of the inner beam (H-pol) slice sampling near the equator for several pulses and antenna rotations on a single ascending pass at a particular location. The 3 dB contour of the slices in the (left) forward-looking and (right) aft-looking direction are shown. The variation in slice shapes between the forward-looking and the aft-looking measurements is apparent.

significant computation and storage requirements since a unique response function is required for each measurement. These requirements are ameliorated by using a tabularized parametric technique for describing the spatial response function.[4] Due to the rapid rolloff and nearly flat mainlobe response of the slices, a significant savings in complexity and computation can be obtained, with only a minor loss in reconstruction accuracy, by quantizing[8] the slice response function to either 1 or 0. Hence for this application, only the shape of the 3 dB contour is required to describe the slice spatial response.[4]

3.2. Reconstruction Theory

In the high resolution wind retrieval approach used here, the goal of the reconstruction algorithm is to extract available information from the measurements to reconstruct higher resolution estimates (images) of the surface σ^o. The resulting σ° images have finer resolution than the 3 dB resolution of the individual slice measurements.

Resolution enhancement algorithms depend on the spatial sampling density of the surface, with finer (denser) sampling resulting in improved resolution. Originally designed only for conventional, low-resolution wind retrieval the SeaWinds instrument is non-optimal for this application (higher azimuth sampling density is desired), but is capable of substantially improved reconstruction-based σ° reconstruction. We note that previous studies[8, 10] have combined multiple passes and azimuth looks to increase the spatial sampling density for land and ice imaging.[2] However, this cannot be used for wind retrieval due to the rapid evolution of the wind-driven surface and the fact that the wind retrieval requires azimuth diversity. Thus, reconstruction of σ° must be done separately for each azimuth look direction to preserve the azimuth diversity of the original measurements. The reconstruction performance is not as good for single-azimuth look, since, as suggested by Fig. 6, the overlap in the measurements is primarily in the along-scan rotation direction; thus the resolution improvement in the reconstructed σ° field is primarily in the along-scan direction. Due to the relative orientations of the measurements, wind retrieval provides the final resolution improvement in the cross-scan direction.

If the sampling and aperture function were uniform and constant, conventional deconvolution techniques could be applied in the reconstruction. Instead, a generalized irregular reconstruction technique is required.[8] One such approach is the scatterometer image reconstruction (SIR) algorithm[8] which was developed especially for scatterometer σ° reconstruction. This algorithm is related to algebraic reconstruction with maximum entropy regularization, but includes a sigmoid non-linearity to reduce the effects of noise.[8] Other reconstruction algorithms can be used. However, in an attempt to limit the required computation, in this paper we adopt use of the simplified AVE[10] algorithm.

The AVE algorithm is the first iteration of the SIR reconstruction and thus is an incomplete reconstruction and can be viewed as a highly regularized reconstruction. While AVE has limited enhancement capability compared to SIR, it is also less noisy.[10] As in both the SIR and AVE algorithms, a fine resolution grid is defined over which σ° is reconstructed. In AVE, the estimated σ° for each grid element (pixel) is computed by averaging the weighted response of all of the measurements covering the pixel, i.e. for each of the four azimuth/polarization looks the estimated σ° at the $(i,j)^{th}$ pixel, $\sigma_{i,j}$, is computed as

$$\sigma_{i,j} = \sum_n h_n(i,j) z_n / \sum_n h_n(i,j) \tag{3}$$

where the summations are over all the measurements n for which $h_n(i,j) \neq 0$. In contrast, the SIR algorithm uses the error in the forward projection to iteratively estimate $\sigma_{i,j}$ from this [Eq. (3)] initial estimate until convergence.[8]

Figure 7 illustrates the pixelization of the spatial response for a particular measurement used in determining the measurements included in the summations in Eq. (3) for each pixel. Figure 7 provides a simple, intuitive example of how averaging within the spatial response function can produce higher effective resolution. This example is considered later.

Experiments suggest that pixels should be sized so that the smallest dimension of a spatial measurement response is a minimum of two pixels wide; however, assuming this minimum requirement is met, the *effective* resolution of the estimates is not dependent on the pixel size. In this paper, the σ° values are estimated on a 2.5 km resolution grid for each of the four beam/look direction combinations: h-pol fore and aft azimuth looks and v-pol fore and aft azimuth looks. Over the outer swath, only v-pol images are created. The cross-track/along-track grid is aligned with the spacecraft groundtrack. In addition to reconstructing the σ° fields, key geometric parameters required for wind retrieval such as the beam azimuth angle are also computed by averaging. The constant incidence angle of SeaWinds simplifies this.

In the swath center, the pixelization of the slice observations can produce isolated pixels which are not (apparently) covered by at least one measurement from each azimuth look. In these cases, in order to simplify

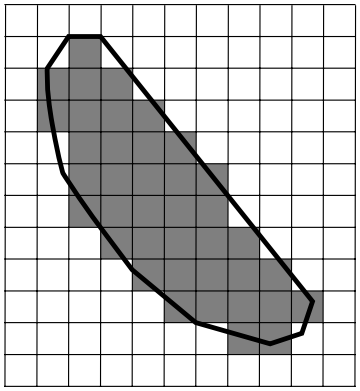

Figure 7. Illustration of a tabularized 3 dB slice contour overlaying an imaging grid. Imaging grid pixels whose centers are contained within the slice contour are shaded to indicate which pixels the slice is considered to have "covered" in the image. Only these pixels are affected by this measurement. Alternate choices of which pixels "belong" to the contour can also be used.[10]

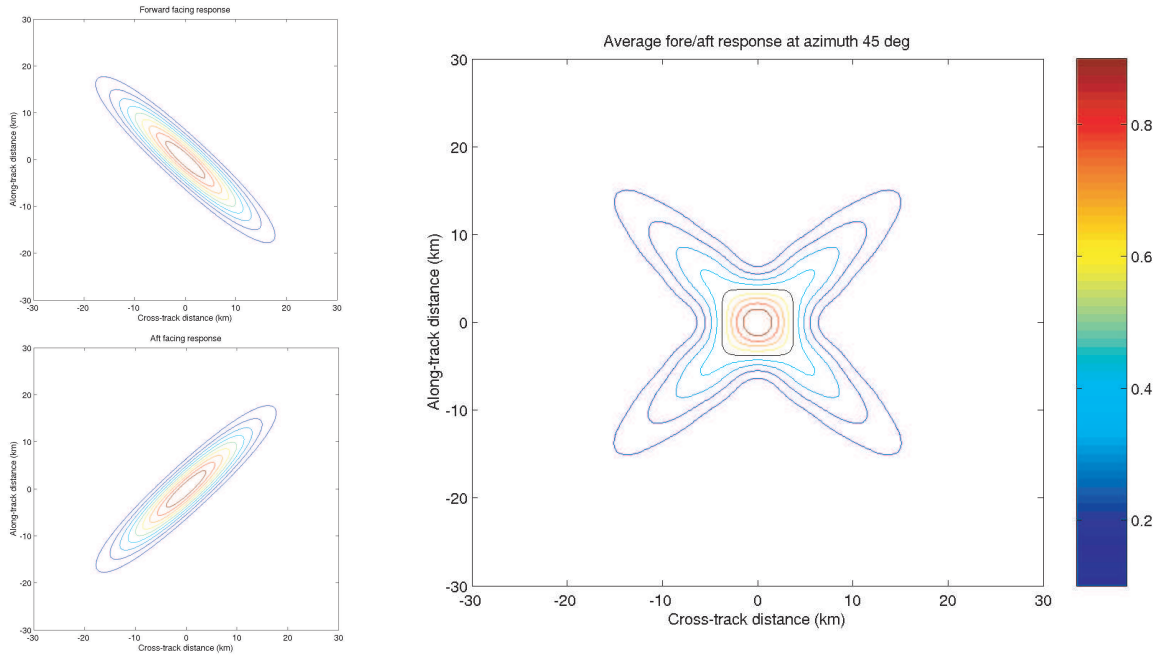

Figure 8. An illustration of how combining overlapping measurements with narrow aspect ratios can yield improved spatial resolution.[6] (left plots) Spatial response functions of two slices corresponding to different azimuth looks. (right plot) Spatial response function resulting from the average of the two measurements to the left. In this example the 3 dB contour (the dark, nearly-square contour in the center) is approximately 8×8 km whereas the original measurements are 8×20 km.

wind processing by ensuring that all pixels within the swath have σ° values, a median hole-filling filter is applied. We note that if the full spatial response were used rather than the quantized slice gain response, this step would not be required.

Figure 9 illustrates these high resolution σ° images generated for one orbit pass over a hurricane. The differences in the elongation of small scale features in the images illustrate the limitations in the incomplete

reconstruction in single azimuth look processing. Given these fields (and the associated geometric information) the effective resolution in the wind estimate is further improved in the non-linear wind estimation algorithm, which in effect acts like a reconstruction algorithm in combining the various azimuth measurements.

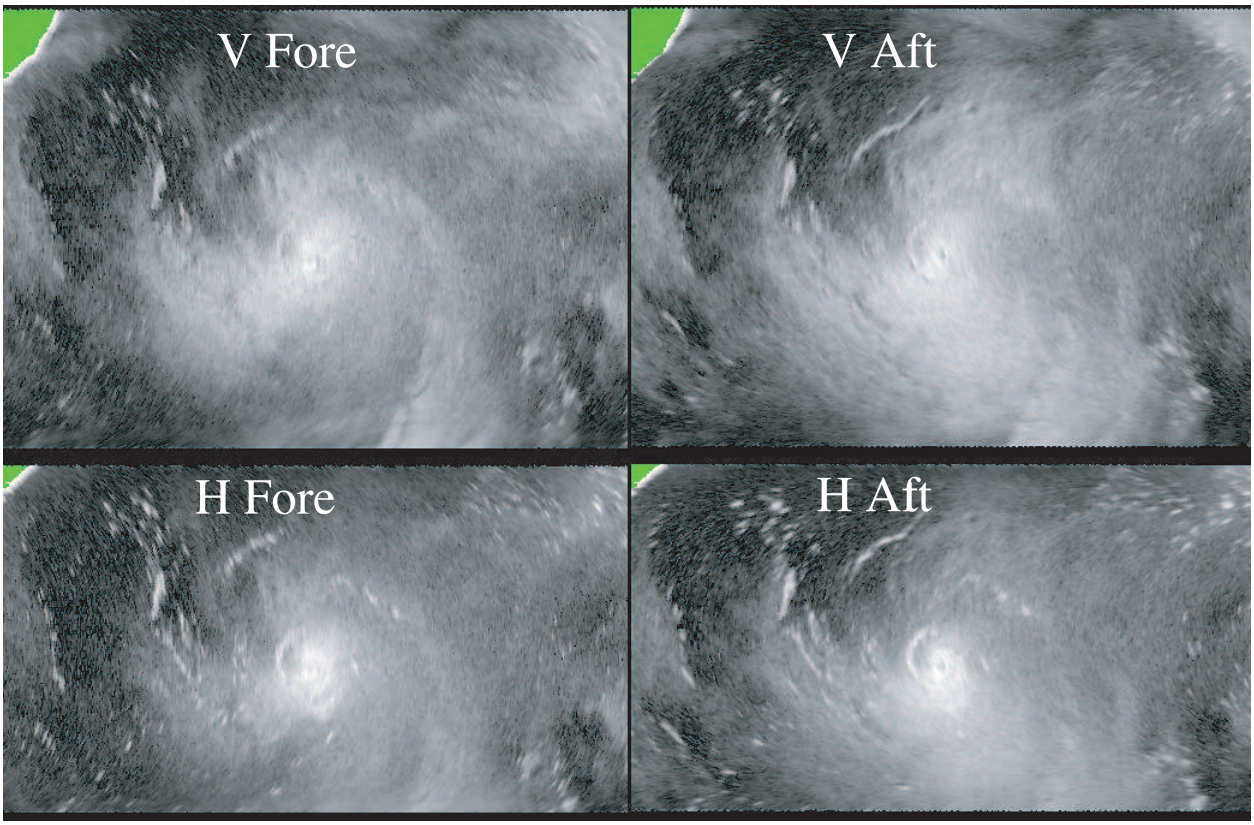

Figure 9. Examples of reconstructed σ° fields from actual SeaWinds slice measurements over Hurricane Isabel in the Atlantic on day 242, 2003 (rev 21848). Approximate north is to the right. σ° is shown in dB. Although not clear in this small reproduction, small scale features such as the hurricane eye are visible. The light spots against the dark background are associated with convective storms. The general brightness of the images are related to wind speed while differences in σ° between the images conveys wind direction information.

3.3. Wind Retrieval

Given the reconstructed σ° values at each high resolution grid point, the wind vector at each pixel is estimated using conventional maximum likelihood wind retrieval techniques.[1] Due to the nature of the geophysical model function, 1-4 ambiguities result. As in conventional estimation, the speeds are similar. In this paper the ambiguity closest to the conventional wind estimate is selected as a first guess. Then, a median-based ambiguity selection algorithm is applied to make the final selection. The result is a spatially consistent, very high spatial resolution, albeit somewhat noisy, estimate of the wind vector field.

In combining reconstructed σ° values from the four azimuth looks, we note that the spatial response functions of reconstructed σ° individual pixels are still long and thin with varying orientation between looks. This variation is exploited in wind estimation to achieve higher spatial resolution measurements by separately retrieving the wind at each pixel. The effective resolution of the resulting wind estimate is a non-linear combination of the individual σ° spatial response functions used to estimate the wind.

Due to the non-linear and non-unique nature of the GMF used in wind retrieval it is difficult to precisely analyze the effective resolution of the retrieved wind. To gain some insight we note that the GMF can be

approximately written as

$$\sigma^o = f(s,\ldots) \approx Gs^H \tag{4}$$

where s is the wind speed and G and H are functions of incidence, azimuth, and polarization with $H \sim 2$. Using the approximation $H = 2$ and ignoring the azimuth dependence of σ^o, a wind-speed only GMF can be written as

$$\sigma^o = \approx Gs^2. \tag{5}$$

While the actual wind retrieval is based on maximum-likelihood, a simple analysis results from the least-squares estimator, $\mathcal{J}(s^2)$, of the squared wind speed s^2

$$\mathcal{J}(s^2) = \sum_n [z_n - f(s,\ldots)]^2 \approx \sum_n [z_n - G_n s^2]^2. \tag{6}$$

The value of s^2 which minimizes $\mathcal{J}(s^2)$ yields the speed estimate. Taking the derivative of $\mathcal{J}(s^2)$ and setting the derivative to zero, the wind speed estimate is,

$$\widehat{s^2} = \frac{\sum_n G_n}{\sum_n G_n^2} z_n = \sum_n b_n z_n \tag{7}$$

where $b_n = \sum_n G_n / \sum_n G_n^2$ is a constant with respect to the wind speed. Thus, the squared-speed estimate is (approximately) a linear combination of the measurements. Unfortunately, a similar simplified analysis for the wind direction estimate has not been developed.

Since squared-speed estimation is approximately linear, conventional analysis can be applied. The effective spatial response function for the wind speed estimate is thus the average of the spatial response functions of the σ° values used. Again, we refer to the illustrative example in Fig. 8 which shows that averaging multiple response functions with thin aspect ratios and variable orientations results in improved resolution of the average. In this application, the inputs are the effective spatial response functions of two reconstructed σ° pixels. Each is from a different azimuth look: one is from a forward-facing measurement, while the second results from a backward-facing measurement (over the inner swath, four azimuth looks are combined). The response functions are long and thin response functions with dissimilar orientations. The 3 dB resolution of the averaged response is much finer than the original observations, and thus has finer spatial resolution, though it has sidelobes reflecting the relative orientation and shapes of the measurements. To first order, the half-power resolution corresponds to the smallest dimension of the input spatial responses.

While a very simplistic analysis, this result suggests that the wind speed (and by implication, the wind direction) estimate resolution is dictated by the area of overlap of the response patterns of the σ° measurements used to retrieve the wind at a given pixel. Subjective examination of the retrieved winds suggests that the effective resolution varies from as fine as 5-6 km to as coarse as 10-12 km over the swath. Since reconstruction tends to enhance the noise along with the resolution, there is a tradeoff between noise and resolution when retrieving the wind at high resolution.

Because the σ° measurements are noisy, the wind estimates are also noisy. Due to the reconstruction, the noise level of the high resolution wind estimates is higher than for conventional resolution winds which are estimated with more measurement averaging. The resulting high resolution wind estimates must thus be used with some care. To reduce the noise in the wind direction estimates for some applications, we retrieve the wind direction at lower resolution by using all the σ° values within a 3×3 window. The direction estimates are combined with the wind direction retrieved at the center of the window.

As previously noted, the wind retrieval algorithm produces from one to four possible wind vectors at each pixel location. The high resolution ambiguity closest to the conventional 25 km wind estimate is selected as a first guess. The conventional winds product contains ambiguity selection errors. While difficult to determine in the conventional products, the selection errors result in visibly discontinuous speed fields, suggesting that it may be possible to use the high resolution wind speeds to check and improve the ambiguity selection in conventional winds. At present, a median-based ambiguity selection algorithm, similar to the one used for conventional processing, is applied to make the final selection. Research to develop improved high resolution ambiguity selection algorithms is underway.

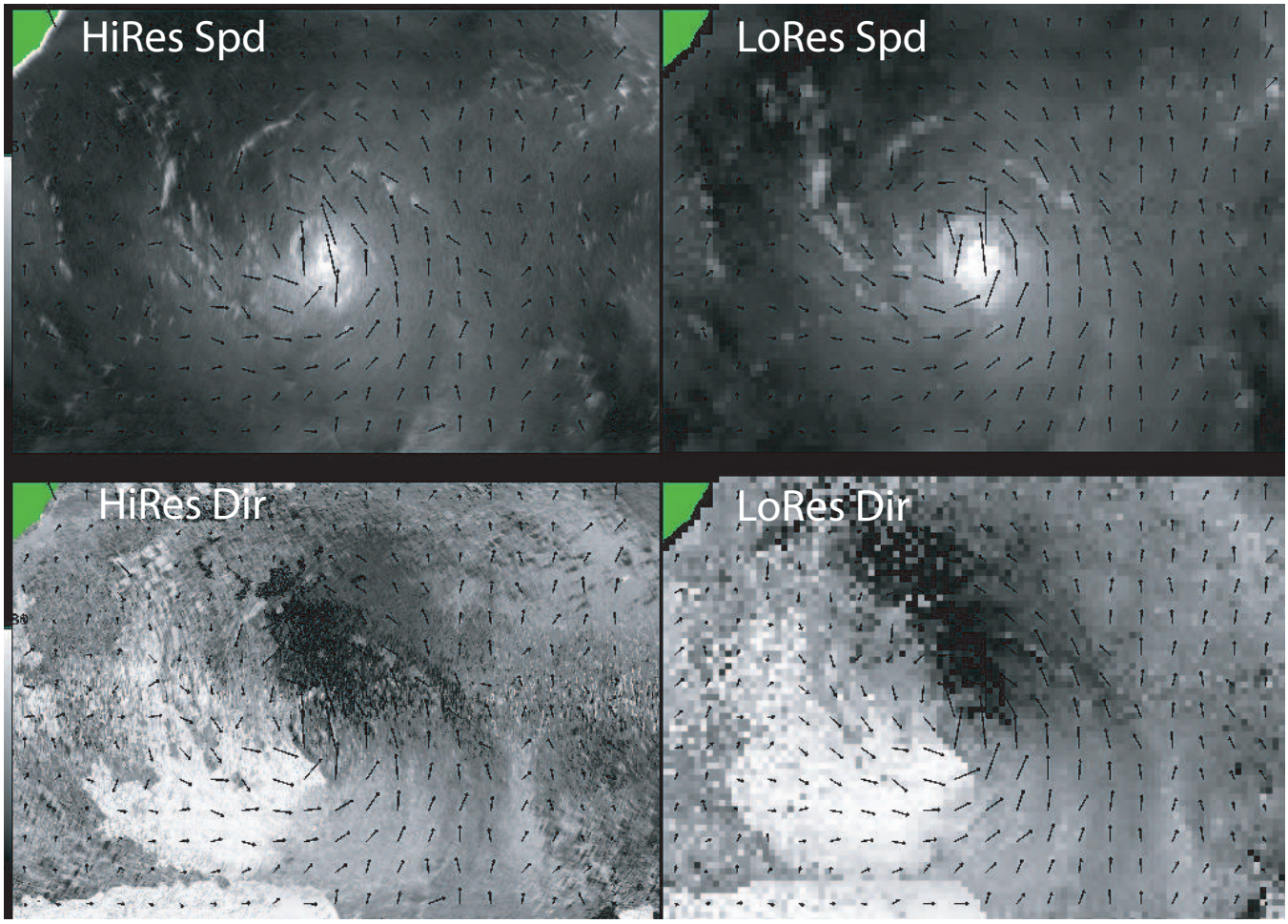

Figure 10. (left column) Wind retrieved on 2.5 km/pixel grid from the σ° in Fig. 9. Approximate north is to the right. (right column) Conventionally retrieved 25 km resolution winds. Note the additional detail apparent in the high resolution fields compared to the low resolution fields. Vector overlays show wind vectors averaged to 250 km resolution.

4. APPLICATION EXAMPLE

Currently, the primary application of high resolution winds is hurricane monitoring, though they are also used in near-coastal, island, and long-term studies. Real-time data from the SeaWinds-on-QuikSCAT mission is operationally being processed into high resolution winds in order to better monitor and track severe weather events such as hurricanes and typhoons. Forecasters are using the high resolution wind information to more precisely locate the eye of the hurricane, a critical factor in track forecasting. Figure illustrates the wind fields retrieved from the high resolution σ° fields previously shown. Note that the hurricane eye and details of the rain bands are more clearly evident in the high resolution fields than in the low resolution fields. Further, what appears to be noise spikes in the low resolution data is resolved into features consistent with mesoscale convective events such as thunderstorms in the high resolution winds.

5. CONCLUSIONS

Though imperfect, high resolution wind estimates can be derived from SeaWinds scatterometer measurements and used in a variety of applications, including near-coastal studies and severe weather and natural hazards

monitoring. High resolution wind capability is a value-added addition to the existing suite of SeaWinds products, which are in use for weather prediction and climate studies.

As one might expect, there is a complex tradeoff between resolution, computation, and noise. Further, the technique is not without limitations: the effective resolution of the estimated wind vectors varies across the swath, and noise in the backscatter measurements is enhanced along with the resolution, leading to noisier wind estimates. Nonetheless, the resulting high resolution winds are now being operationally used for weather prediction and monitoring hurricanes and severe storms. Although high resolution winds from SeaWinds must be used with care due to their limitations (since the instrument was not originally designed for this application), future missions can be designed with these techniques in mind to achieve significantly better wind measurement performance. Further, improvements to the processing algorithms can also be envisioned.

ACKNOWLEDGMENTS

QuikSCAT data was obtained from the Physical Oceanography Distributed Data Archive (PO.DAAC) at the CalTech Jet Propulsion Laboratory.

REFERENCES

1. F. Naderi, M. Freilich, and D. Long, "Spaceborne radar measurement of wind velocity over the ocean–an overview of the NSCAT scatterometer system," *Proc. IEEE* **79**(6), pp. 850–866, 1991.
2. D. Long, M. Drinkwater, B. Holt, S. Saatchi, and C. Bertoia, "Global ice and land climate studies using scatterometer image data," *EOS, Trans. American Geophysical Union* **82**(43), p. 503, 23 Oct. 2001.
3. M. Spencer, C. Wu, and D. Long, "Improved resolution backscatter measurements with the SeaWinds pencil-beam scatterometer," *IEEE Trans. Geosci. Remote Sens.* **38**(1), pp. 89–104, 2000.
4. I. Ashcraft and D. Long, "The spatial response function of SeaWinds backscatter measurements," in *Earth Observing Systems VIII*, W. L. Barnes, ed., *Proc. SPIE* , 2003.
5. I. Ashcraft, D. Long, A. Anderson, S. Richards, M. Spencer, and B. Jones, "Sigma-0 retrieval from SeaWinds on QuikSCAT," in *Earth Observing Systems IV*, W. L. Barnes, ed., *Proc. SPIE* **3750**, pp. 171–179, 1999.
6. D. Long and J. Luke, "High resolution wind retrieval for SeaWinds," in *Ocean Remote Sensing and Imaging II*, R. Frouin, G. Filbert, and D. Pan, eds., *Proc. SPIE* **5155**, pp. 216–225, 2003.
7. P. Yoho and D. Long, "Correlation and covariance of satellite scatterometer measurements," *IEEE Trans. Geosci. Remote Sens.* **42**(6), pp. 1176–1187, 2004.
8. D. Early and D. Long, "Image reconstruction and enhanced resolution imaging from irregular samples," *IEEE Trans. Geosci. Remote Sens.* **39**(2), pp. 291–302, 2001.
9. F. Ulaby, R. Moore, and A. Fung, *Microwave Remote Sensing: Active and Passive*, vol. 2, Artech House, Inc., Norwood, Massachusetts, 1986.
10. D. Long, P. Hardin, and P. Whiting, "Resolution enhancement of spaceborne scatterometer data," *IEEE Trans. Geosci. Remote Sens.* **31**(3), pp. 700–715, 1993.